Acta Crystallographica Section B
Structural Science
ISSN 0108-7681

Structure of caesium disulfate at 120 and 273 K

Kenny Ståhl,* Rolf W. Berg, K. Michael Eriksen and Rasmus Fehrmann

Technical University of Denmark, Department of Chemistry, DK-2800 Lyngby, Denmark

Correspondence e-mail: kenny@kemi.dtu.dk

Received 27 January 2009
Accepted 22 July 2009

The crystal structures of $Cs_2S_2O_7$ at 120 and 273 K have been determined from X-ray single-crystal data. Caesium disulfate represents a new structure type with a uniquely high number of independent formula units at 120 K: In one part caesium ions form a tube surrounding the disulfate ions, $[Cs_8(S_2O_7)^{6+}]_n$; in the other part a disulfate double-sheet sandwiches a zigzagging caesium ion chain, $[Cs_2(S_2O_7)^{6-}]_n$. Caesium disulfate shows an isostructural order–disorder transition between 230 and 250 K, where two disulfate groups become partially disordered above 250 K. The Cs^+-ion arrangement shows a remarkable similarity to the high-pressure Rb^{IV} metal structure.

1. Introduction

The most widely used catalyst for SO_2 oxidation in sulfuric acid production is a molten $M_2S_2O_7$–V_2O_5 mixture supported by a kieselguhr carrier under reaction conditions (Topsøe & Nielsen, 1947). Classically M is approximately a 1:3 Na:K mixture as for instance in the VK 38 and WK WSA industrial catalysts by Haldor Topsoe A/S, which acts as a solvent for the catalytically active vanadium complexes. Recently the phase diagram of the $Na_2S_2O_7$–$K_2S_2O_7$ system was constructed based on combined conductivity measurements, thermal measurements and classical thermodynamic calculation (Rasmussen *et al.*, 2001), together with the crystal-structure determinations of $Na_2S_2O_7$ and $KNaS_2O_7$ (Ståhl *et al.*, 2005). In some specialized catalysts, such as VK 59 and VK 68 by Haldor Topsoe A/S, small amounts of Cs are added to the $M_2S_2O_7$–V_2O_5 mixture as a third alkali promoter. It is therefore interesting to also investigate $Cs_2S_2O_7$-containing model catalyst systems. This work presents the X-ray single-crystal structures of $Cs_2S_2O_7$ at 120 and 273 K, as well as their Raman spectra.

2. Experimental methods

2.1. Sample preparations

$Cs_2S_2O_7$ was prepared by thermal decomposition of $Cs_2S_2O_8$ (Merck, p.a.) at 523 K over 3 h. $Cs_2S_2O_7$ single crystals were grown from zone melting ten times in an evacuated, sealed, fused quartz tube. The colourless, hygroscopic disulfate salt was stored in vacuum-sealed Pyrex ampoules, and when opened handled in dry N_2 atmosphere in a glove-box throughout the preparations, and in a flow of dry N_2 during X-ray data collection.

Table 1
Caesium coordination in $Cs_2S_2O_7$.

Central atom	Coordination No.	Shortest distance (Å)	Longest distance (Å)	Average distance (Å)†	$\sigma(2)$‡	Ecc§	Valence sum§
(*a*) At 120 K							
Cs0	8	2.916 (7)	3.516 (7)	3.186 (2)	0.20	0.096	1.14
Cs1	10	2.961 (6)	3.607 (6)	3.271 (2)	0.23	0.035	1.18
Cs2	9	3.018 (6)	3.238 (6)	3.169 (2)	0.07	0.027	1.21
Cs3	8	2.976 (6)	3.473 (7)	3.180 (2)	0.16	0.054	1.10
Cs4	10	3.089 (5)	3.577 (6)	3.304 (2)	0.15	0.037	0.98
Cs5	9	3.104 (6)	3.426 (5)	3.253 (2)	0.12	0.037	0.99
Cs6	9	2.968 (7)	3.341 (6)	3.198 (2)	0.12	0.025	1.15
Cs7	9	3.001 (6)	3.466 (6)	3.251 (2)	0.18	0.030	1.05
Cs8	11	3.049 (6)	3.586 (7)	3.293 (2)	0.17	0.024	1.14
Cs9	9	3.064 (6)	3.418 (6)	3.232 (2)	0.12	0.026	1.05
Cs10	10	3.060 (5)	3.514 (6)	3.272 (2)	0.15	0.040	1.08
Cs11	11	3.126 (6)	3.626 (6)	3.378 (2)	0.16	0.054	0.90
Cs12	8	2.966 (6)	3.307 (7)	3.136 (2)	0.11	0.032	1.20
Cs13	9	3.059 (6)	3.435 (6)	3.245 (2)	0.10	0.018	1.00
Cs14	9	2.962 (6)	3.362 (7)	3.205 (2)	0.12	0.060	1.13
Cs15	11	3.136 (6)	3.541 (7)	3.301 (2)	0.13	0.052	1.08
Cs16	9	2.997 (6)	3.516 (7)	3.219 (2)	0.20	0.090	1.17
Cs17	11	2.993 (6)	3.564 (6)	3.268 (2)	0.17	0.065	1.22
Cs18	8	2.984 (7)	3.496 (6)	3.123 (2)	0.18	0.045	1.30
Cs19	10	2.929 (6)	3.620 (7)	3.291 (2)	0.27	0.078	1.19
(*b*) At 273 K							
Cs1	10.5	2.945 (34)	3.611 (26)	3.317 (4)	0.18	0.048	1.03
Cs3	9	3.101 (11)	3.513 (11)	3.299 (4)	0.15	0.031	0.90
Cs5	8.5	2.711 (14)	3.572 (20)	3.225 (5)	0.20	0.080	1.14
Cs7	9	3.039 (14)	3.598 (11)	3.238 (4)	0.18	0.037	1.08
Cs9	9	3.021 (10)	3.622 (15)	3.245 (4)	0.18	0.037	1.07
Cs11	9	2.925 (10)	3.652 (12)	3.253 (4)	0.25	0.029	1.14
Cs13	8	2.876 (15)	3.548 (36)	3.261 (5)	0.19	0.041	0.93
Cs15	10.5	2.993 (32)	3.615 (21)	3.356 (4)	0.19	0.066	0.95
Cs17	10	3.022 (9)	3.618 (13)	3.304 (4)	0.23	0.079	1.07
Cs19	8.5	2.837 (19)	3.650 (20)	3.2241 (4)	0.28	0.078	1.21

† $\sigma(1) = (\Sigma_i \sigma_i^2)^{1/2}/n$. ‡ $\sigma(2) = [\Sigma_i (d_i - \langle d \rangle)^2/(n-1)]^{1/2}$. § Eccentricity and valence sums calculated using *IVTON* (Balić-Žunić & Vicković, 1996) and averaged over the disordered O sites.

Table 2
Disulfate geometries in $Cs_2S_2O_7$.

Disulfate No.	Terminal S—O (Å)	Bridging S—O (Å)	S—O—S angle (°)	Twist angle (°)†
(*a*) At 120 K				
0	1.434 (3)	1.641 (4)	126.4 (4)	8.7 (3)
1	1.443 (2)	1.644 (4)	128.1 (3)	15.9 (2)
2	1.432 (3)	1.642 (4)	123.3 (4)	54.1 (3)
3	1.436 (2)	1.640 (4)	123.4 (3)	52.2 (3)
4	1.440 (2)	1.640 (4)	124.0 (3)	4.4 (3)
5	1.441 (2)	1.650 (4)	123.1 (3)	50.4 (2)
6	1.443 (2)	1.638 (4)	122.6 (3)	30.7 (2)
7	1.445 (2)	1.638 (4)	121.6 (3)	44.0 (2)
8	1.436 (3)	1.632 (4)	123.3 (4)	59.2 (3)
9	1.438 (2)	1.640 (4)	122.0 (3)	39.3 (3)
(*b*) At 273 K				
1*A*	1.428 (7)	1.612 (8)	130 (2)	8.2 (1.3)
1*B*	1.430 (6)	1.658 (12)	128 (1)	6.6 (1.0)
3	1.429 (4)	1.625 (5)	122.8 (4)	44.8 (4)
5	1.423 (4)	1.634 (6)	123.4 (5)	47.6 (4)
7	1.418 (4)	1.639 (5)	124.3 (4)	50.9 (4)
9*A*	1.432 (5)	1.620 (5)	124.9 (5)	9.0 (6)
9*B*	1.429 (5)	1.620 (5)	124.9 (5)	50.8 (7)

† The twist angles are calculated as the average of the three smallest O—S—S—O torsion angles.

2.2. Single-crystal data collection, structure solution and refinements

Two colourless crystals of $Cs_2S_2O_7$ were selected for the single-crystal data collection on a Bruker SMART APEX diffractometer at 120 and 273 K. The final results from the two crystals were identical and the datasets chosen for presentation were the ones that gave the lower final standard errors. The data were checked for crystal decay by remeasuring the first 50 frames of data after completed data collection, but revealed no crystal decay for any of the crystals. The refinement tested for extinction, but the extinction coefficient was insignificantly different from zero. Several oxygen sites were found severely disordered at 273 K showing unrealistically short S—O distances. In disulfate group 1 all the oxygen sites were split in two, as for one sulfate tetrahedron in disulfate group 9. These split oxygen positions were refined with isotropic displacement parameters and the S—O and O—O distances restrained to ideal values. With ten split oxygen sites, 486 parameters and 58 restraints $wR(F^2)$ was reduced to 0.164 compared with a non-split model with all anisotropic atoms resulting in $wR(F^2)$ of 0.166 using 496 parameters. The displacement parameters of sulfate group 1 are still quite high, indicating a more complex disorder, which could not be resolved at the present level of resolution. The numbering of the atomic sites has used the following rules: C*sn*, where n = 0–15 refers to the tube structure and n = 16–19 refers to the sandwich structure. In the disulfate groups, S*nm* and O*nm*, n = 0–1 refers to the tube structure and n = 2–9 refers to the sandwich structure, m = 1–2 is sulfur, m = 3 is the bridging oxygen, and m = 4–9 are the terminal O atoms. At 273 K all *n*s are odd, at 120 K even numbers are generated by the phase transition so that numbers 0 and 1, 2 and 3 and so on at 120 K collapse into the odd numbers when compared with the 273 K structure. The split O-atom positions at 273 K are given the labels *A* and *B* for connected tetrahedral sets. The final atomic parameters are available as supplementary material,[1] selected averaged distances and angles in Tables 1 and 2, and the structures are illustrated in Figs. 1–3. Experimental details are summarized in Table 3.

2.3. Unit-cell determinations

A 0.15 × 0.14 × 0.07 mm single crystal was used for unit-cell determinations in the temperature range 120–270 K. The crystal was first heated from 120 to 240 K in steps of 20 K using

[1] Supplementary data for this paper are available from the IUCr electronic archives (Reference: BP5020). Services for accessing these data are described at the back of the journal.

approximately 30 min per step; the temperature was kept at 240 K for another 20 min before remeasuring and then heating continued to 250 and 270 K. After standing overnight, the crystal was cooled down to 190 K in steps of 10 K. The data between 120 and 230 K were indexed as the low-temperature unit cell from, on average, 400 reflections. All 240 K datasets gave unreasonable unit cells (axis lengths between 62 and 121 Å). The data from 250 K gave both the low- and high-temperature unit cells, the 260 K data the high-temperature

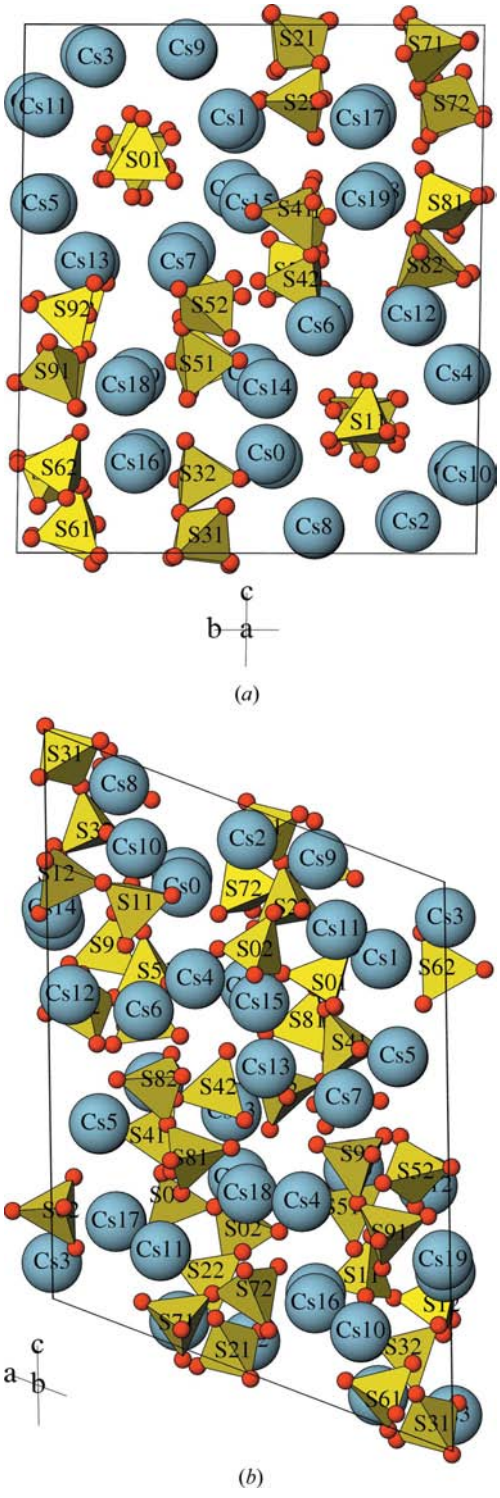

Figure 1
Projection of $Cs_2S_2O_7$ at 120 K projected along (*a*) the *a* axis and (*b*) the *b* axis. Cs ions are shown as large spheres and the disulfate ions as polyhedra.

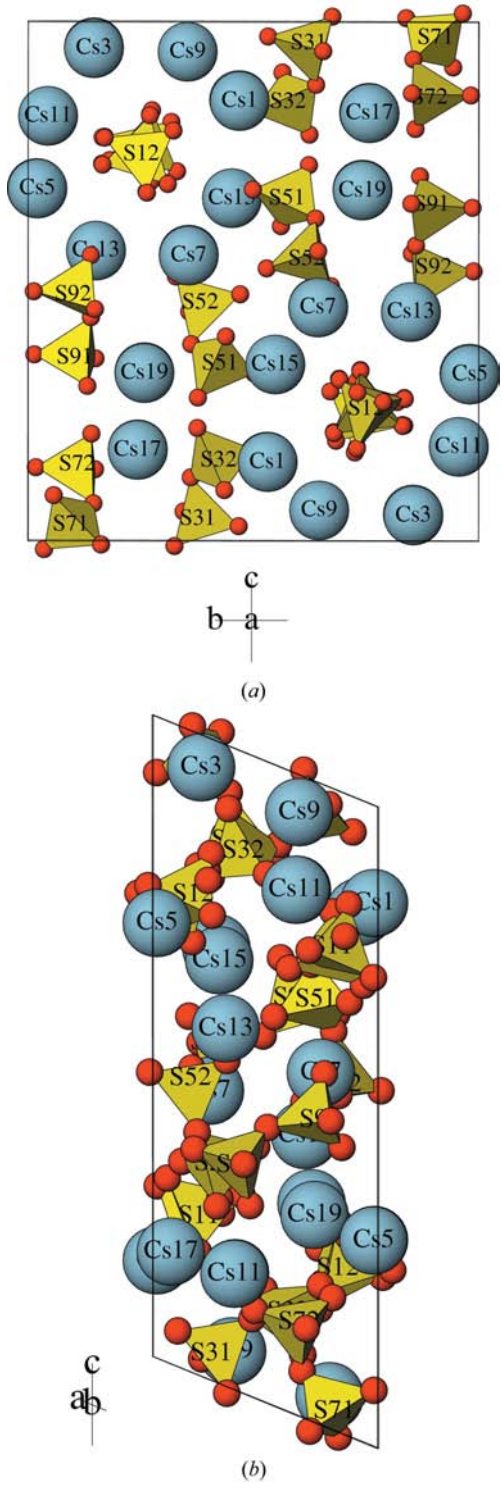

Figure 2
Projection of $Cs_2S_2O_7$ at 273 K projected along (*a*) the *a* axis and (*b*) the *b* axis. Cs ions are shown as large spheres and the disulfate ions as polyhedra.

unit cell and the 270 K data at first an unreasonable unit cell and then the high-temperature unit cell after standing overnight. The high-temperature datasets were indexed from, on average, 270 reflections. The results are shown in Fig. 4 as relative changes of a selection of unit-cell parameters, where the high-temperature unit cells were transformed to the low-temperature cells for the sake of comparison.

2.4. Raman spectroscopy

Sampling was carried out in small melting-point capillary tubes filled with a few needles of the crystals and sealed. Raman spectra were measured using a DILOR-XY 800 mm focal length multi-channel spectrometer. Spectra were excited with an Ar^+-ion laser (514.5 nm wavelength, $\sim$ 300 mW and with plasma lines filtered off by an interference filter). The Rayleigh scattered light was filtered off using a double pre-monochromator or a Kaiser SuperNotch-Plus holographic filter (approximately 200 cm^{-1} cut-off), giving spectra looking identical. The Raman light was dispersed using an 1800 lines mm^{-1} grating in the 800 mm focal-length single spectrograph and focused on the CCD detector. The slits were set to 200 µm, corresponding to a resolution of $\sim$ 5 cm^{-1}. The precision was $\sim$ 1 cm^{-1} for sharp bands, achieved by calibration using crystalline S_8, liquid cyclohexane and neon emission lines superimposed on the spectra. The Raman spectra are shown in Fig. 5 and a list of Raman bands is given in Table 3.

2.5. Differential scanning calorimetry

Data were collected on a Perkin–Elmer Pyris Diamond DSC. The sample (50.7 mg) was enclosed in a gold ampoule prepared in a glove-box and measured from 213 to 743 K at

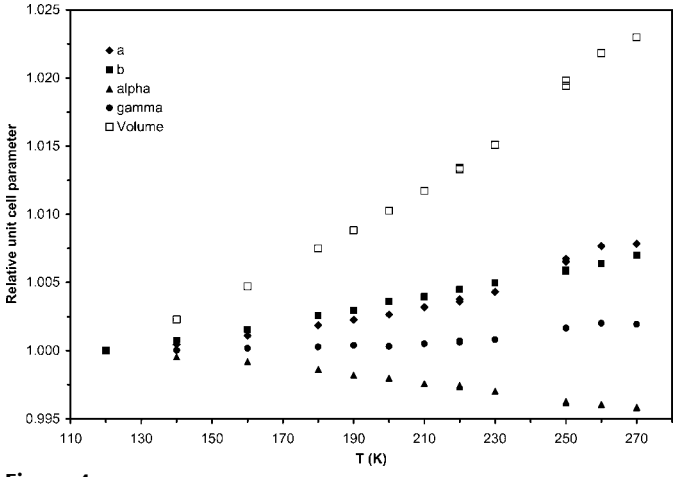

Figure 4
Relative unit-cell dimensions *versus* temperature. The 250, 260 and 270 K high-temperature unit cells were transformed to the low-temperature unit cells for the sake of comparison. Standard errors are on average 0.0001.

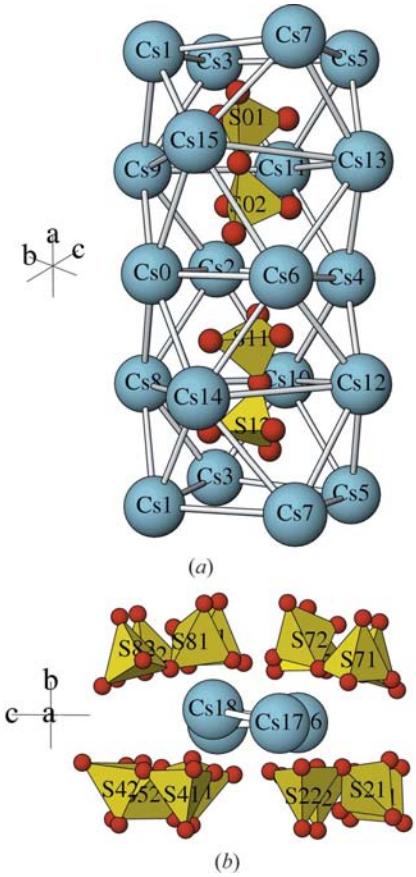

Figure 3
Perspective drawings of (*a*) the Cs tube with enclosed disulfates in $Cs_2S_2O_7$ at 120 K, (*b*) the sandwich structure in $Cs_2S_2O_7$ at 120 K. Cs(*n*) and S(*nm*) sites with even *n*s are generated by symmetry in the 273 K structure. The Cs–Cs connections are added as a guide to the eye.

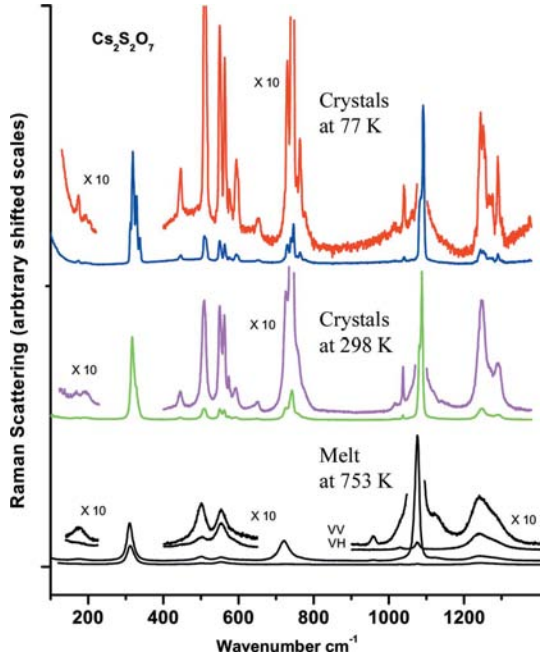

Figure 5
Raman spectra of $Cs_2S_2O_7$ at 77, 298 and 753 K. Polarized (VV) and depolarized (VH) spectra are shown for the melt (753 K). Selected ranges are also shown magnified ×10 and displaced vertically.

Table 3
Experimental details.

	120 K	273 K
Crystal data		
Chemical formula	$Cs_2S_2O_7$	$Cs_2S_2O_7$
M_r	441.96	441.96
Crystal system, space group	Triclinic, $P\bar{1}$	Triclinic, $P\bar{1}$
a, b, c (Å)	14.9411 (16), 16.0362 (17), 19.300 (2)	7.5229 (5), 15.9592 (10), 19.4841 (12)
α, β, γ (°)	85.025 (2), 67.630 (2), 74.968 (2)	85.3100 (10), 67.2880 (10), 77.7750 (10)
V (Å^3)	4129.5 (8)	2108.9 (2)
Z	20	10
Radiation type	Mo $K\alpha$	Mo $K\alpha$
μ (mm^{-1})	9.32	9.13
Crystal form, size (mm)	Irregular, 0.11 × 0.10 × 0.06	Plate, 0.11 × 0.10 × 0.06
Data collection		
Diffractometer	Bruker SMART APEX	Bruker SMART APEX
Data collection method	ω scan, frame data integration	ω scan, frame data integration
Absorption correction	Multi-scan†	Multi-scan†
T_{min}, T_{max}	0.404, 0.411	0.572, 0.578
No. of measured, independent and observed reflections	55 593, 23 807, 19 521	28 312, 12 178, 9077
Criterion for observed reflections	$I > 2\sigma(I)$	$I > 2\sigma(I)$
R_{int}	0.032	0.033
θ_{max} (°)	31.0	31.0
Refinement		
Refinement on	F^2	F^2
$R[F^2 > 2\sigma(F^2)]$, $wR(F^2)$, S	0.051, 0.115, 1.06	0.067, 0.164, 1.07
No. of reflections	23 807	12 178
No. of parameters	991	486
$(\Delta/\sigma)_{max}$	0.008	0.001
$\Delta\rho_{max}$, $\Delta\rho_{min}$ (e Å^{-3})	10.58, −5.20	4.87, −5.11

Computer programs used: *SMART* (Bruker, 1998*a*), *SAINT-Plus* (Bruker, 1998*b*), *SHELXS*97, *SHELXL*97 (Sheldrick, 2008), *ATOMS*6.1 (Dowty, 2000). † Based on symmetry-related measurements.

5 K min^{-1}, kept at 743 K for 10 min and then from 743 to 293 K at 5 K min^{-1}. The resulting curve is shown in Fig. 6.

3. Discussion

The crystal structures of inorganic dianion salts, $M_a(X_2O_7)_b$, can in most cases be divided into two types: thortveitite-like and dichromate-like (Clark & Morley, 1976). For instance, the previously known alkali disulfate structures, $Na_2S_2O_7$, $NaKS_2O_7$ and $K_2S_2O_7$, all show dichromate-like structures (Ståhl *et al.*, 2005). However, the crystal structure of $Cs_2S_2O_7$ represents a novel structure type (Figs. 1–3). It can be described as built from two larger building blocks: a Cs tube enclosing disulfate ions, $[Cs_8(S_2O_7)^{6+}]_n$ (Fig. 3*a*); and a disulfate double sheet structure sandwiching a Cs zigzag chain, $[Cs_2(S_2O_7)_4^{6-}]_n$ (Fig. 3*b*). The formation of these blocks may be envisaged as templating processes, where disulfates and Cs ions guide the formation of the Cs tubes and the sandwich structure. The isostructural phase transition between 230 and 250 K (see below) is of the order–disorder type. At 273 K the disulfate ions labelled 1 and 9 are disordered. The disordered disulfates are described with split O-atom positions giving alternative SO_4 tetrahedra orientations (*cf.* Table 2*b* and Fig. 2). On cooling to 120 K the unit-cell volume is doubled, while retaining the $P\bar{1}$ symmetry, and is accompanied by a specific volume reduction of 2.1%. The relationship between the two unit cells is: $a_{120\,K} = 2a_{273\,K}$, $b_{120\,K} = b_{273\,K}$, $c_{120\,K} = c_{273\,K}$. The phase transition thus doubles the number of independent atoms in the structure and all atomic positions are found to be ordered at 120 K. The structures have a uniquely high number of independent atoms for such simple stoichiometry: 110 atoms at 120 K and 55 atoms at 273 K.

Comparing Figs. 1(*a*) and 2(*a*) the extent of positional splitting is clearly seen. From Table 2 it is seen that the tube disulfates 0 and 1 are essentially in an eclipsed conformation (the O—S—S—O torsion angle < 30°), but pack in a staggered fashion with respect to each other. At 273 K the disordered disulfate 1 is an equal and random mixture of the 120 K disulfates. The other disordered disulfate (9) results in splitting into one eclipsed and one staggered conformation. The eclipsed disulfate 4 and the staggered disulfate 5 at 120 K transform into one staggered disulfate at 273 K. The remaining disulfates are essentially unaltered during the phase transition. The largest splitting of Cs positions is seen for Cs14 and Cs15 (∼ 0.9 Å), which can be directly related to a combination of the splitting of the staggered ordered disulfate 5 at 273 K into the eclipsed disulfate 4 and staggered disulfate 5 at 120 K, and the ordering of disulfate 1. The mixture of staggered and eclipsed disulfates and the transformations between them are in contrast and transformations between them are in contrast to the uniformity of the thortveitite- and dichromate-like structures, where the dianions are either all staggered or all eclipsed, respectively (Clark & Morley, 1976). Obviously the interaction with the Cs arrangement imposes this variation in the disulfate conformations. Theoretical calculations on the disulfate ion in the gas phase have shown that the equilibrium conformation is partly staggered with C_2 symmetry (Dyekjær *et al.*, 2003), which is the approximate conformation found in the majority of disulfates in the present structure. The eclipsed conformation, *syn*-C_{2v}, was shown to be 12.23 kJ mol^{-1} higher in energy. The ideally staggered conformation with C_s symmetry is only 1.52 kJ mol^{-1} higher in energy than the C_2 conformation (Dyekjær *et al.*, 2003), indicating that thermal energy plays a significant role in structural rearrangements and disorder in the disulfate groups. The observed S—O—S angles are on average 126°, which is consistent with the dichromate-like

Table 4
Raman bands for $Cs_2S_2O_7$.

Band positions are given in cm^{-1}. Intensity code: w = weak; m = medium; s = strong; sh = shoulder; v = very; dp = depolarized.

Raman, crystal at 81 K	Raman, crystal at 298 K	Raman melt at 753 K
1293 w	1295 vw	1278 w,br,dp
1279 vw	1274 vw	1240 w,br,dp
1270 vw	1251 w	1128 w,br,p
1260 vw		
1255 w		
1246 w		
1233 vw		
1094 vs	1091 s	1078 vs,p
1086 m, sh	1084 m, sh	1072 m,p
1043 w	1040 w	1032 w,dp
1018 vw		(961.6 w,p)
779 vw	758 vw	761 w,br,p or dp
766 w	744 m	723 m,p
758 vw	728 w	
748 s		
741 m		
732 m		
658 vw	653 vw	
653 vw		
602 w	595 w	590 vw,?
595 w	576 vw	555 w,dp
578 vw	563 w	503 w,p
566 w	552 w	
552 w	510 w	
516 m		
509 m		
447 w	446 vw	447 vw,p
338 m	329 w, sh	314 s,dp
330 s	318 s	
320 vs		
314 s		
207 vw	193 vw	178 w,p
195 vw	169 vw	
175 w		

structures (Clark & Morley, 1976). The S—O—S angles show a slight increase when going from the staggered to the eclipsed conformation, which is also predicted from the theoretical calculations (Dyekjær *et al.*, 2003).

It is not always straightforward to find the *M*—O coordination number when *M* is an alkali metal ion owing to the irregular polyhedra formed (Ståhl *et al.*, 2005). In the present case the Cs—O coordination limits were identified as significant jumps to the next coordination distance, when a Cs—S distance was the next in line, or when the sum of covalent radii plus 0.5 Å was exceeded. The average Cs coordination geometries are given in Table 1, where in the 273 K dataset (Table 1*b*) weighted averages of the two conformations (*i.e.* four conformation sets) were used. The Cs—O coordination number varies between 8 and 11 at 120 K, and between 8 and 10.5 at 273 K. The Cs—O coordinations show a general positive correlation between the average coordination distance and the coordination number. There is an increase in the average coordination distances of 0.027 Å when going from 120 to 273 K. This expansion can be attributed to the overall thermal expansion and to increased librational motion of the disulfate groups, resulting in shorter S—O and longer Cs—O average distances. The average valence sums at 120 and 273 K are 1.11 and 1.05, respectively, again a consequence of the temperature-induced increase in Cs—O distances. The valence sums show no correlation to Cs—O distances or coordination numbers, which indicate overall well conditioned coordinations. However, there is a noticeable difference between the valence sums of the tube and sandwich Cs ions, being on average 0.12 higher for the sandwich Cs ions. It can be seen as an effect of generally more distorted Cs—O coordinations in the sandwich part when looking at the spread in coordination distances [$\sigma(2)$ in Table 1] and eccentricity. An increased distortion owing to the exponential nature of the bond-valence-to-distance relationship results in such an increase.

Two attempts to establish a more precise phase-transition temperature were made: unit-cell determinations between 120 and 270 K on a single crystal, and DSC measurements between 213 and 743 K on a polycrystalline sample. The single-crystal data indicated a phase-transition temperature between 230 and 250 K (Fig. 4), with notable jumps in the α and γ parameters and an inflection point at $\sim$ 240 K in the volume curve. The transition appears sluggish and possibly involves kinetically hindered microtwinning or microdomain formation. Neither a more precise transition temperature nor reaction order was possible to establish using DSC (Fig. 6). However, the DSC curve revealed a second phase transition at 434 K on heating and 410 K on cooling, indicating a first-order transition. The ΔS value was calculated as 6.61 and 6.27 J mol^{-1} K^{-1}, corresponding to $R\ln 2 = 5.76$ J mol^{-1} K^{-1} of an order–disorder transition. Transforming the 273 K unit cell according to $a' = a$, $b' = b$ and $c' = -a + c$ results in $a' = 7.5229$ (5), $b' = 15.959$ (1), $c' = 17.973$ (1) Å, $\alpha = 90.207$ (1), $\beta = 90.418$ (1), $\gamma = 102.206$ (1)°, *i.e.* transformation to a monoclinic high-temperature phase cannot be ruled out.

Further attempts to characterize the phase transition were made by Raman spectroscopy (Fig. 5). The spectrum of crystals at room temperature showed the expected bands owing to vibrational transitions in the $S_2O_7^{2-}$ ion, as discussed in detail

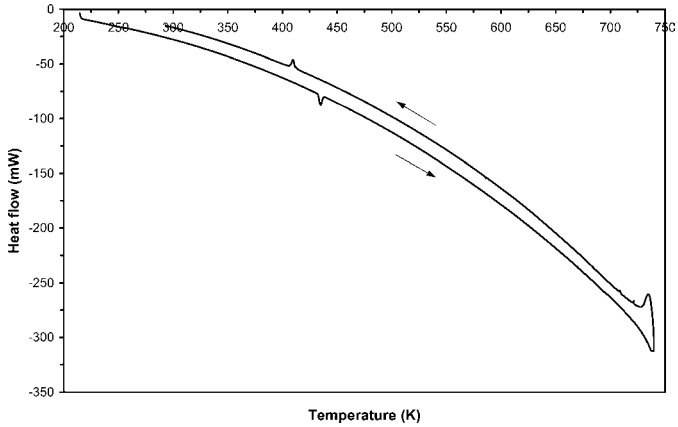

Figure 6
DSC on $Cs_2S_2O_7$. Exothermic reaction is up.

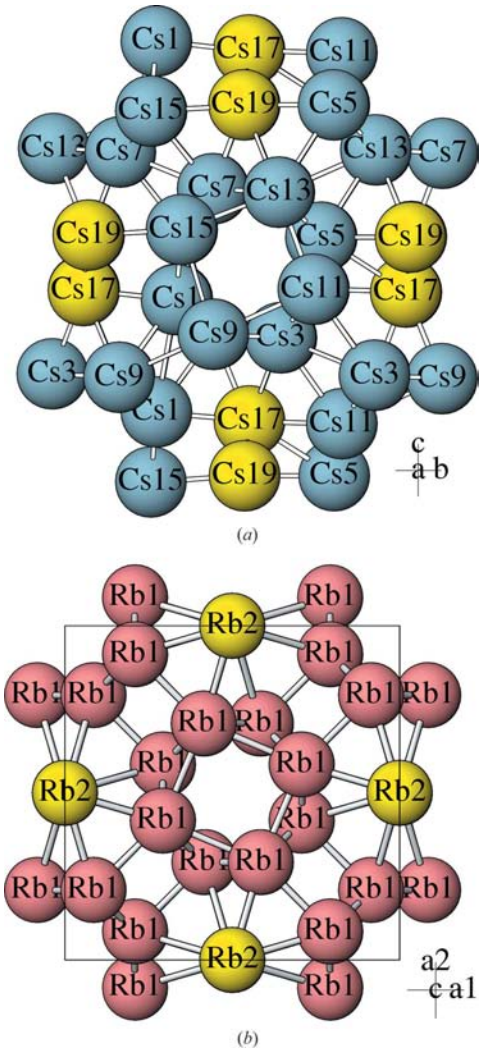

Figure 7
Comparison of (*a*) the Cs arrangement in the $Cs_2S_2O_7$ structure and (*b*) the Rb^{IV} structure.

in Dyekjær *et al.* (2003). These bands are very distinct in the melt spectra (Fig. 5). Owing to the sluggish nature of the phase transition it was not possible to establish the transition temperature by methods previously used (Berg, 1978). Unfortunately, the phase transition in the present system does not seem to affect the spectrum, except for sharpening the bands. Such sharpening has been observed in many other cases, see for instance Berg & Adams (1981). The spectral bands are listed in Table 4.

An interesting comparison of the present structure and that of several high-pressure metal structures can be made: considering only the Cs positions (Fig. 7*a*), there is a striking similarity between this structure and the high-pressure Rb^{IV} structure (Fig. 7*b*; Schwarz *et al.*, 1999). The host structure of Rb^{IV} corresponds to the Cs tube structure, while the often incommensurate guest atoms in Rb^{IV} correspond to the zigzagging Cs band in the sandwich structure. However, the metal–metal distances are very different, 3.0–3.3 Å in Rb^{IV} and 4.3–5.9 Å in $Cs_2S_2O_7$. The host structure appears in several electronically different high-pressure metal structures as for example Sr^{V}, Ba^{IV}, Bi^{III} and Sb^{II} (Schwarz, 2004), and one may speculate whether or not it represents a generally favourable packing principle.

4. Conclusions

The crystal structure of caesium disulfate has a novel structure type with a uniquely high number of independent formula units in the asymmetric unit. The arrangement of the Cs^{+} ions shows a remarkable similarity to Rb^{IV} high-pressure metal structure. Between 230 and 250 K caesium disulfate shows an isostructural order–disorder transformation. The transformation temperature was determined from the unit cell change, but appeared sluggish and could not be observed by DSC or Raman spectroscopy.

The authors are grateful to Ms Astrid Schøneberg and Ms Lize Lotte Berring for patient X-ray data collections and Ms Bodil Holten for DSC data collections. Support by Corrit Foundation, Tuborg Brewery Foundation, Danfoss A/S, Thomas B. Thrige Foundation, P. A. Fiskers Foundation, Direktør Ib Henriksens Foundation is gratefully acknowledged.

References

Balić Žunić, T. & Vicković, I. (1996). *J. Appl. Cryst.* **29**, 305–306.
Berg, R. W. (1978). *J. Chem. Phys.* **69**, 1325–1335.
Berg, R. W. & Adams, D. M. (1981). *J. Mol. Struct.* **71**, 17–21.
Bruker (1998*a*). *SMART*, Version 5.054. Bruker Analytical X-ray Instruments Inc., Madison, Wisconsin, USA.
Bruker (1998*b*). *SAINT*, Version 5.054. Bruker Analytical X-ray Instruments Inc., Madison, Wisconsin, USA.
Clark, G. M. & Morley, R. (1976). *Chem. Soc. Rev.* **5**, 269–295.
Dowty, E. (2000). *ATOMS*, Version 6.1. Shape Software, Kingsport, USA.
Dyekjær, J. D., Berg, R. W. & Johansen, H. (2003). *J. Phys. Chem. A*, **107**, 5826–5830.
Rasmussen, S. B., Eriksen, K. M., Hatem, G., da Silva, F., Ståhl, K. & Fehrmann, R. (2001). *J. Phys. Chem. B*, **105**, 2747–2752.
Schwarz, U. (2004). *Z. Kristallogr.* **219**, 376–390.
Schwarz, U., Grzechnik, A., Syassen, K., Loa, I. & Hanfland, M. (1999). *Phys. Rev. Lett.* **83**, 4085–4088.
Sheldrick, G. M. (2008). *Acta Cryst.* A**64**, 112–122.
Ståhl, K., Balić-Žunić, T., da Silva, F., Eriksen, K. M., Berg, R. W. & Fehrmann, R. (2005). *J. Solid State Chem.* **178**, 1697–1704.
Topsøe, H. F. A. & Nielsen, A. (1947). *Trans. Dan. Acad. Technol. Sci.* **1**, 18–24.